THE USE OF ELECTRICAL RESISTIVITY TOMOGRAPHY TO INVESTIGATE THE SUBSURFACE LITHOLOGY IN UGBOGIOBO TOWN, OVIA NORTH EAST LOCAL GOVERNMENT AREA OF EDO STATE.

BY

OSENI RESAQ ABU

PSC1607934

A PROJECT WRITTEN IN THE DEPARTMENT OF PHYSICS AND SUBMITTED TO THE DEPARTMENT OF IN PARTIAL FULFILMENT OF THE REQUIREMENT FOR THE AWARD OF BACHELOR OF SCIENCE DEGREE IN PHYSICS, UNIVERSITY OF BENIN, BENIN CITY, NIGERIA.

JUNE, 2021.

CERTIFICATION

I hereby certify that this project was carried out under my supervision by **OSENI RESAQ ABU,** a final year student of Department of Physics, Faculty of Physical Sciences, University of Benin, Benin City, Edo State, Nigeria.

---------- ----------

PROF M. O. ALILE Date
Supervisor

---------- ----------

DR. O. D. OSAHON Date
Ag.Head of Physics Department

....

EXTERNAL EXAMINER Date

DEDICATION

This project is dedicated to ALMIGHTY GOD for His love, provision, mercies and protection all through my years in school and also to my family and friends/colleagues.

ACKNOWLEDGEMENT

I sincerely express my profound gratitude to ALMIGHTY GOD for his protection, favor, grace and mercy upon my life, for being there for me throughout the period of this research work. Special thanks goes to my project supervisor M. O. Alile for his understanding and fatherly advice, May God reward you handsomely sir.

I also want to appreciate my parents Mr. and Mrs Oseni Aneru for supporting me financially, spiritually and physically to achieve my goals; May the good lord grant you good health to enjoy the fruit of your labour. To my siblings, Oseni Raheem, Osdeni Aminat, Oseni Nurudeen, I say thank you all.

To my course mates I appreciate all your efforts towards the completion of this project. I pray God perfect all that concerns you.

ABSTRACT

2-D survey of a part of Ugbogiobo community and its environs has been carried out successfully and this research has helped in providing information about the subsurface of the study area. This information is of utmost importance as it gives the necessary constituents of the profile of the study area. The subsurface of a study area is related to various geological parameters such as mineral and fluid content, porosity and degree of water saturation in the rock.

Major resistivity structures were delineated in both profile which is seen to be generally characterized by moderate resistivity values, at the top layers we can inferred from the low resistivity that is characterize by Clayey and Alluvium soil having a resistivity range between 200 Ωm – 800 Ωm profile 7 and 8 respectively. The major mineral occurrence in profile 7 and 8 are majorly compose of sedimentary Rocks ranging from Limestone, Shale and Sandstone with a resistivity range for Limestone between 2000 Ωm – 3000 Ωm, Shale with a resistivity range 3200 Ωm – 4000 Ωm Sandstone between resistivity range 4000 Ωm – 5000 Ωm, it will be noticed from the profiled line that all inferred mineral types fall between a depth of 2 m to 39 m. which form the lithological mineral occurrence of the both profiles.

The development of two dimensional inversion resistivity algorithms has aided the processing and interpretation of complex data. Due to the inferred rock types and mineral occurences (Alluvium, Clayey soil, limestone, sandstone, and clay) gotten from the lithological interpretation of the 2-D data inversion, it can be concluded that the lithology of the study area is good for engineering purpose and construction work.

TABLE OF CONTENT

CHAPTER FIVE

LIST OF FIGURES

LIST OF TABLES

CHAPTER ONE

INTRODUCTION

1.1 ELECTRODE CONFIGURATIONS

The term 'electrode configuration' simply refers to the arrangement patterns or methods of placement of electrodes on the earth surface during electrical resistivity survey. There are numerous electrode configurations which can be used in the arrangement of electrodes by geophysicists. These different arrays have particular advantages, disadvantages and their difference in sensitivity to anisotropy. Factors affecting the choice of array type include the amount of space available to layout an array, the labour-intensity of each method, the sensitivity to lateral inhomogeneities (Habberjam and Watkins, 1967; Barker, 1981) and to dipping interfaces (Broadbent and Habberjam, 1971). Another important factor in the choice of array is the simplicity of the expression of the geometric factor, *K.* For example, one of the simplest geometric factor expressions is that of the well-known Wenner arrangement, $K = 2\pi a$ where *a* is the distance between the equally spaced electrodes *A, M, N,* and *B (A* and *B* are current electrodes; *M* and *N* are potential electrodes). In the Schlumberger array, the geometric factor, *K,* is more complex and is given by$K = \pi\,[(AB/2)^2 - (MN/2)^2]\big/MN$, where $AB \geq 5MN$. The importance of this geometric factor, *K,* cannot be overemphasized, as it determines

the measured apparent resistivity. In practice, one or more tables of precalculated values for K are used to facilitate the computation of the apparent resistivity, ρ_a from the well-known general formula

$$\rho_a = K \Delta V / I \tag{1.1}$$

where ΔV is the measured voltage (between M and N) and I is the electric current. For a given distance between current electrodes, AB, and a given current intensity, J, one measures a smaller potential difference, ΔV when using the Schlumberger array than when using the Wenner array. This is mathematically expressed in an inverse relationship for the corresponding geometric factors. Thus more current is required when using the Schlumberger than when using the Wenner array to produce the same ΔV at the same AB. However, the sensitivity of the Schlumberger array for detecting a given layer, at a given depth and at a given AB, is greater than that of the Wenner array (Deppermann, 1954: Zohdy, 1964).

In recent years, the possibility of making electrical soundings using dipole-dipole arrays has received considerable attention (Alekseev et al, 1957; Anderson and Keller, 1966; Cantwell et al, 1965; Cantwell and Orange, 1965; Berdichevskii, 1957; Al'pin, 1950 Berdichevskii and Zagarmistr, 1958; Jackson, 1966). In general, the value of the geometric factor for any quadruple array can be computed from the Equation (1.1) which will be derived in the chapter two of this work.

$$K = 2\pi\left(\frac{1}{r_1} - \frac{1}{r_2} - \frac{1}{r_3} + \frac{1}{r_4}\right)^{-1} \quad (1.2)$$

where r_1, r_2, r_3 and r_4 are the distances *AM, AN, BM,* and *BN* between the current electrodes, *A* and *B,* and the potential electrodes, *M* and *N* as shown in the diagram below.

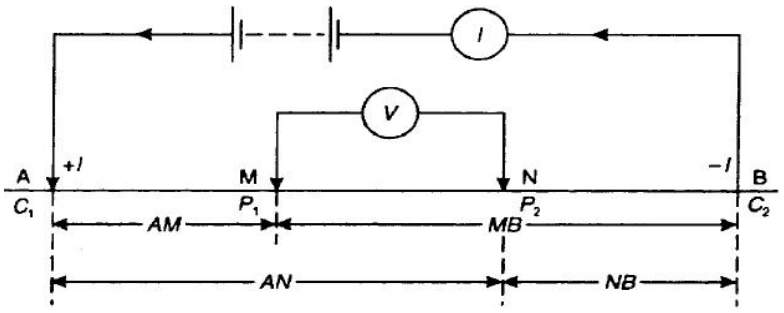

Figure 1.1: A diagram showing the general form of electrode configuration for resistivity surveying.

All resistivity arrays, when classified based on sensitivity to anisotropy, are divided into two groups: collinear arrays (Schlumberger, Wenner, pole-pole, pole-dipole, dipole axial) with the axes ratio equal λ, and non-collinear arrays (dipole equatorial, T-array, etc.) with sensitivity up to λ^5. Most sensitive to inclined contact is dipole axial array, and it is the least sensitive to anisotropy (Dr. Evgueni Pervago, 2001).

1.2 ELECTRODE SPREAD

Many electrode configurations have been designed. Although several of them are occasionally employed in specialized surveys, only five (5) would be explained in

this project work and that is, the Schlumberger, Wenner, dipole-dipole and pole dipole arrays for 1D and 2D electrical resistivity surveys.

1.2.1 Two-Dimensional Imaging Methods

The most commonly used arrays for 2-D imaging surveys are (i) Wenner-Schlumberger, (ii) Schlumberger, (iii) pole-pole, (iv) pole-dipole and (v) dipole-dipole.

1.2.1.1 Wenner Method

This is a robust array type which was popularized by the pioneering work carried by the University of Birmingham research group (Griffiths and Turnbull, 1985; Griffiths, Turnbull and Olayinka, 1990). The Wenner array maintains a constant spacing between the electrodes as shown in Figure 2.5. It is best suited for profiling because only one electrode is moved for measurements. Beard and Morgan (1991) found that the expanding electrodes of the Wenner array create false analomous zones that complicate interpretation. Figure 2.4 (b) shows that the sensitivity plot for the Wenner array has almost horizontal contours beneath the center of the array. So, the Wenner array is relatively more sensitive to vertical changes than to horizontal changes in subsurface resistivity. Furthermore, the Wenner array has a moderate depth of investigation compared to the other arrays. As seen in Table 2.2, the median depth of investigation for Wenner array is

approximately 0.5 times the spacing used. The geometric factor for Wenner array is $2\pi a$. The geometric factor is smaller when compared to all other arrays.

Wenner array has the strongest signal strength among all the arrays because the potential electrodes are placed between the two current electrodes. The disadvantage of this array for 2-D imaging surveys is it has relatively poor resolution as spacing between the electrodes is increased. This method cannot take advantage of multi-channel system as only single channel is used during the testing.

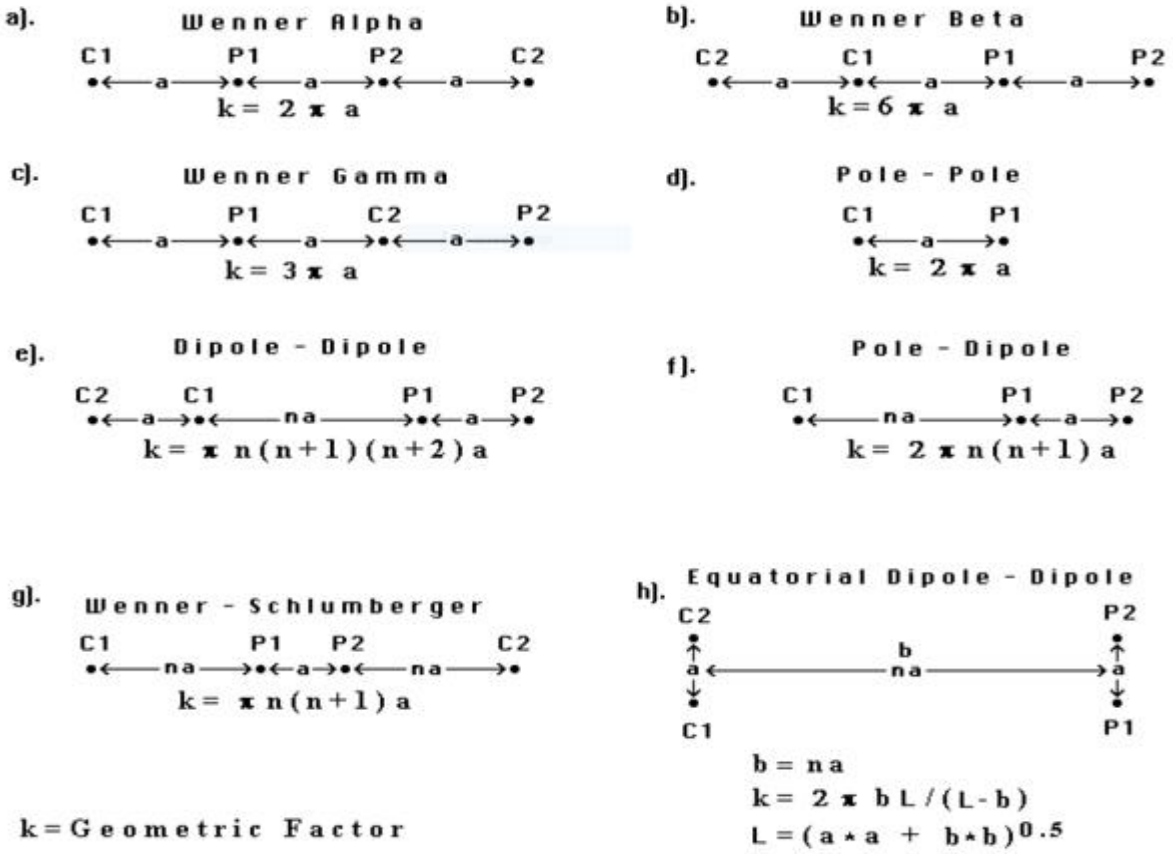

Figure 1.2: Common arrays used in resistivity surveys and their geometric factors.

1.2.1.2 Wenner-Schlumberger Method

One of the first arrays used in the 1920's and still popular today is the Schlumberger array. The most commonly used array for resistivity sounding surveys is Schlumberger array. This array can be used on a system by arranging the electrodes with a constant spacing as shown in Figure 2.5. The "**n**" factor for this array is the ratio of the distance between the C1-P1 (or P2-C2) electrodes and the spacing between the P1- P2 potential pair. The sensitivity patterns of Schlumberger array and Wenner array vary slightly. The Schlumberger array is moderately sensitive to both horizontal and vertical structures which has a slight vertical curvature below the centre of the array, and also has slightly lower sensitivity values in the regions between the C1 and P1, C2 and P2 electrodes. Hence, the Schlumberger array might be a good compromise between the Wenner and the dipole-dipole array in the areas where both horizontal and vertical structures are expected. The signal strength of Wenner array is high and the signal strength of Schlumberger array is between Wenner array and dipole–dipole array. When compared to the Wenner array, the median depth of investigation (with the same distance between the outer (C1 and C2) electrodes) is about 10 % larger for Schlumberger array.

1.2.1.3 Dipole-dipole Method

The dipole-dipole array is logistically the most convenient in the field, especially for the work over large areas and larger spacing's between the electrodes. Dipole-dipole provides the highest resolution and is most sensitive to vertical resistivity boundaries

(Griffiths and Barker, 1993). However, the data collected from dipole-dipole array are easily affected by near-surface resistivity variations (Griffiths and Barker, 1993). Figure 2.7 shows the data collection sequence for the dipole-dipole array in an ERT investigation. The symbol "a" denotes the unit spacing of electrodes, which is selected based on the desired depth of penetration, the required resolution, and the type of array. The electrode spacing and dipole separation are constant for each traverse (*n*) and increases with each successive traverse. Larger electrode spacing provides data from greater depths, but with poor resolution.

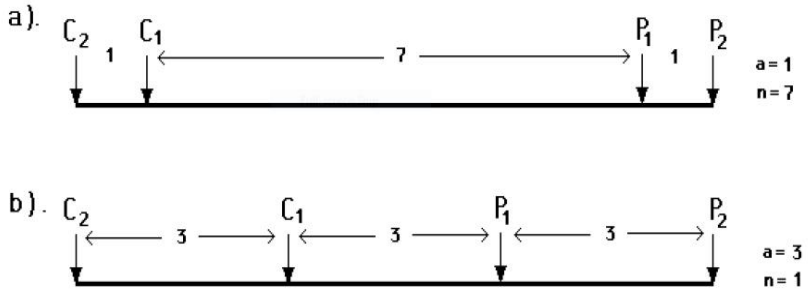

Figure 1.3: Two different arrangements for a dipole-dipole array measurement (Loke, 1999).

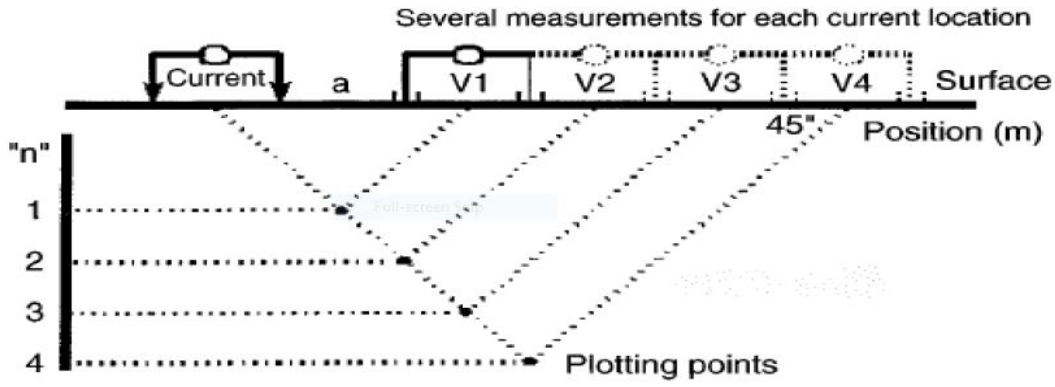

Figure 1.4: Data measurement sequence using dipole-dipole array (Zhou, 1999).

1.2.1.4 Pole-dipole Method

The pole-dipole array is an asymmetrical array (Figure 1.4), unlike the other common arrays and over symmetrical structures the apparent resistivity anomalies are asymmetrical in the pseudosection. In some cases, the model obtained after inversion can be influenced by the asymmetry in the measured apparent resistivity values. The effect of the asymmetry can be eliminated by repeating the measurements by arranging the electrodes in the reverse order. With the combination of "forward" and "reverse" pole-dipole arrays, any bias in the model caused by the asymmetrical nature of the array can be removed. The signal strength of pole-dipole array is significantly higher when compared to the dipole-

dipole array and also the pole-dipole array is not as sensitive as pole-pole array to telluric noise, but the pole-dipole array has relatively good horizontal coverage.

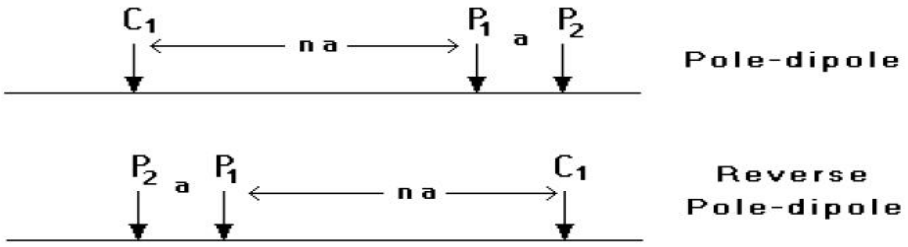

Figure 1.5: Forward and reverse pole-dipole arrays (Loke, 1999)

The pole-dipole array requires a remote electrode, the C2 electrode. The distance between this electrode and the survey line should be sufficiently far. For the pole-dipole array, the effect of the C2 electrode is approximately proportional to the square of ratio of the C1-P1 distance to the C2-P1 distance. Hence the pole-dipole array is less affected by the C2 remote electrode when compared to the pole-pole array. If the distance of the C2 electrode is more than 5 times the largest C1-P1 distance used, the error caused by neglecting the effect of the C2 electrode is less than 5%.

1.2.1.5 Pole-Pole Method

This array is not as commonly used as the Wenner, dipole-dipole and Schlumberger arrays. In practice the ideal pole-pole array, with only one current and one potential electrode, does not exist. To approximate the pole-pole array, the second current and potential electrodes (C2 and P2) must be placed at a distance

that is more than 20 times the maximum separation between C1 and P1 electrodes used in the survey. The effect of the C2 (and similarly for the P2) electrode is approximately proportional to the ratio of the C1-P1 distance to the C2-P1 distance. It is popular in some applications such as archaeological surveys where small electrode spacings are used. It has also been used for 3-D surveys (Li and Oldenburg 1992). This array has the widest horizontal coverage and the deepest depth of investigation. However, it has the poorest resolution, which is reflected by the comparatively large spacing.

2.3 ADVANTAGES, LIMITATIONS AND APPLICATIONS OF ELECTRICAL RESISTIVITY METHODS

2.3.1 Advantages

i. Non-invasive: No digging or large scale drilling is required
ii. Acquisition is relatively straightforward
iii. Processing is automated
iv. Can provide relatively high- resolution 2-D or 3-D conductivity images of subsurface
v. The equipment is light, portable and inexpensive

Table 1.1: Properties of electrode arrays (Bernard, 2004)

Common	**Topsoil**	50 – 100

rocks	**Loose sand**	500 – 5000
	Gravel	100 – 600
	Clay	1 – 100
	Weathered bedrock	100 – 1000
	Sandstone	200 – 8000
	Limestone	500 – 10 000
	Greenstone	500 – 200 000
	Gabbro	100 – 500 000
	Granite	200 – 100 000
	Basalt	200 – 100 000
	Graphitic schist	10 – 500
	Slates	500 – 500 000
		500 – 800 000
Ore	**Pyrites (ores)**	1.01 – 100
minerals	**Pyrrhotite**	0.001– 0.01
	Chalcolpyrite	0.005 – 0.1
	Galena	1.01 – 100
	Sphalerite	1000 – 1 000 000
	Magnetite	0.01– 1000
	Cassiterite	0.001– 10 000

	Hematite	0.01– 1 000 000

2.3.2 Disadvantages

i. Deep investigations require long cables and consume much field time

ii. Interpretation of complex geologic structures is difficult and ambiguous

iii. Presence of metal pipes, cables, fences and electrical grounds can complicate interpretation.

2.3.3 Limitations

i. Interpretations are ambiguous. Consequently, independent geophysical and geological controls are necessary to discriminate between valid alternative interpretations of the resistivity data.

ii. Interpretation is limited to simple structural configurations. Any deviations from these simple situations may be impossible to interpret.

iii. Topography and the effects of near-surface resistivity variations can mask the effects of deeper variations.

2.3.4 Applications

The various applications of Electrical Resistivity are:

i. Location of sources of ground water targets.

ii. Mapping saline water intrusion and contaminant plumes.

iii. Locating the depth of buried foundations of ancient buildings and structures.

iv. Depth to bedrock.

v. Estimating landfill thickness

vi. Map stratigraphy

2.4 BENEFITS OF 2D ELECTRICAL RESISTIVITY METHOD

One of the principle advantages of 2D resistivity reviews over 1D techniques like VES is the effortlessness. However, the advantages don't exclusively lie in the overview's usability. The genuine advantage of a two-dimensional resistivity overview over a one-dimensional resistivity study is that it's undeniably more exact and simpler to decipher. Think about the earth like a portion of bread. At the point when you lead a 2D geophysical resistivity study, you are making one cut through the bread, start to finish. In case you're looking for an irregularity—to stay with our bread model, a raisin leading a 2D review will give you a sign of the area of the raisin (for example the irregularity) Advanced Geosciences, Inc. (AGI).

1.5 AIM AND OBJECTIVE

The aim of this work is to investigate the subsurface lithology of the study area in order to ensure if the subsurface of the study area is fit to withstand massive structures and road networks.

The objective of this work are to;

1. To obtain a 2 dimensional model of the sub surface by inverting the observed data set.
2. To infer from the 2 dimensional model, the rock formation in the sub surface from which one can tell if the terrain is suitable for environmental and engineering studies.

1.6 LOCATION OF SURVEY AREA

This work was carried out in Ebomisi Secondary School located in Ugbogiobo Town, Ovia North East Local Government Area of Edo State. The Wenner Alpha array was use.

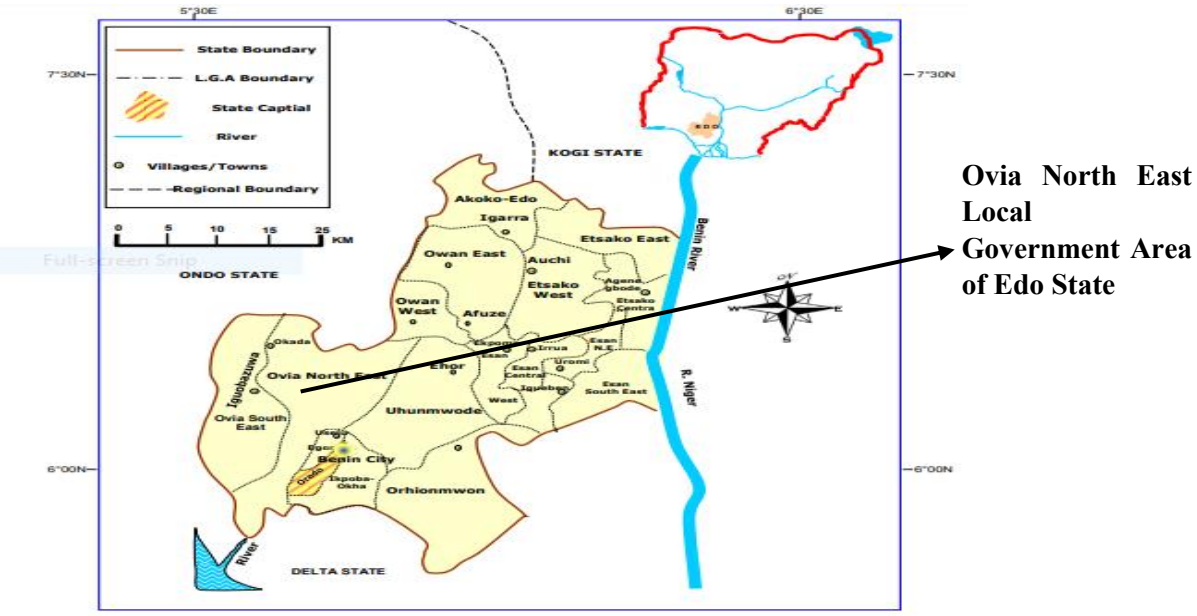

Figure 1.6: Map of Edo state showing the study area

1.7 GEOLOGY OF STUDY AREA

The various formations in the geology of Edo State are: Benin, Bende Ameki, Ogwashi-Asaba, Imo and Nsukka. The geology of the study area is characterized by deposits laid during the tertiary and cretaceous periods. The area is underlain by sedimentary rock constituting part of the Benin formation which is made up of over 90% massive, porous, coarse sand with thick clay/shale interbeds having high groundwater retention capacity. Soil particles vary from coarse grained to fine grained in some areas, poorly sorted, sub-angular well-rounded particles with lignite streaks and fragments.

However reinstated the name Benin formation to identify the reddish-brown-yellow generally white sands often with clayey and pebbly horizons with type-locality around Benin. This is also referenced at Calabar and other parts of South Eastern Nigeria. The formation was further established by well logging of Etete 1, well drilled on-shore east of River Niger by Shell Nigeria. Petroleum Development Company (SPDC) and described by. The formation is about 1830 m thick at the seashore but thins landwards. The sedimentary suits of the Benin Formation dip 2˚ - 8˚ south. Geologically, the Benin Region comprises of 1) the Benin formation; 2) alluvium; 3) drift/top soil and 4) Azagba-Ogwashi (Asuba-Ogwashi) formation.

1.7.1 The Benin Formation

It is assigned to the Oligocene-Pleistocene period in the continent of Africa and to the Oligocene-Pleistocene recent at the sub-oceanic. The formation is characterized by top reddish to reddish brown lateritic massive fairly indurate clay and sand. This is often marked with reticulate muderacks. This caps the underlying more friable pinkish-yellowish white often gravelly-pebble sands clayey soils, sands and clay. The sedimentary sequences are poorly bedded with discontinuous clay horizons at various depths. It is estimated to be about 800m thick under Benin City and about 1,830m near the sea shore sections of the formation. They are

exposed at various erosion sites, sand quarry sites, and road cuttings. The Benin formation covers 95% of the region.

1.7.2 Alluvium

These are found along Ikpoba and Ovia flood plains. They are made up of grayish-dirty white-yellowish-white sands, silts, clayey sands, gravels and even wood-plant materials. These have been washed down the river valley and deposited at the river banks. They are recent deposits.

1.7.3 Drift/Top Soil

Drifts are sediments still in the process of transportation or movement. They are made up of light brown-yellowish silt, mudflows and sands derived from the weathering of the parental Benin Formation. Drifts are washed down by fluvial agents especially the storms and floods dominating the wet season of the region. The drifts are not part of the solid geology. But they are mainly derived and reworked materials and loads dropped by moving floods. Drifts cover roadsides; fill up areas, concealing the underlying geology. Drifts vary from very thin.

CHAPTER TWO

LITERATURE REVIEW

2.1 GENERAL CONSIDERATION OF DC RESISTIVITY SURVEYS

In resistivity surveying, information about the subsurface distribution of electrical conductivity is obtained by examining how currents flow in the earth. DC (direct current) resistivity methods involve injecting a steady state electrical current into the ground and observing the resulting distribution of potentials (voltages) at the

surface or within boreholes. Like all geophysical processes, DC surveys can be described in terms of input energy, the earth's physical properties, and signals or data that are measured.

Figure 2.1: Describing DC survey

The energy source is a pair of electrodes that inject a well-known current into the ground at known locations. The earth affects this energy because variations in the electrical conductivity of subsurface structures will bend the current flow lines. The measured signals or data will involve measurements of voltage at the earth's surface or within boreholes. This type of data contains information about how charges become distributed at boundaries where electrical conductivity changes.

For each placement of the transmitting electrodes, several voltages will often be measured at different locations. Therefore, the complete data set includes measured voltages with known currents and electrode geometries. In order to create maps or graphs of raw data for quality assessment or for direct interpretations, it is usual to convert the data into a form that has units of resistivity. Such results are most commonly used as the input for DC resistivity inversions, in which the results will be 1D, 2D or 3D models of how subsurface conductivity is distributed.

2.2 THE PHYSICAL PROPERTY - ELECTRICAL CONDUCTIVITY

Electrical conductivity (or resistivity) is a bulk property of material describing how well that material allows electric currents to flow through it. Consider current flowing through the unit cube of material shown to the right. The electrical conductivity of Earth's materials varies over many orders of magnitude. It depends upon many factors, including: rock type, porosity, connectivity of pores, nature of the fluid, and metallic content of the solid matrix. Soils and rocks are composed mostly of silicate minerals, which are essentially insulators. Exceptions include magnetite, specular hematite, carbon, graphite, pyrite, and pyrrhotite. Therefore, conduction is largely electrolytic, so conductivity depends mainly upon:

- Porosity;
- Hydraulic permeability, which describes how pores are interconnected;
- Moisture content;
- Concentration of dissolved electrolytes;
- Temperature and phase of pore fluid;
- Amount and composition of colloids (clay content).

2.3 CURRENT FLOW IN THE GROUND

The path of the current in the earth after it is injected with two electrodes depends upon the distribution of electrical resistivity. If the Earth is uniform, current flows in a regular three dimensional pattern under the electrodes as illustrated Figure 1. The north slice number 8 (flagged with a *) is similar to the type of image

commonly shown in texts to indicate how current flows in two dimensions under a pair of source electrodes.

2.3.1 Sources

High power and reliable constant current are the primary requirements of DC resistivity transmitters. For small scale work (electrodes up to roughly 100 m apart), a transmitter capable of sourcing up to several hundred milliwatts of power might be adequate. For larger scale work (electrodes as much as 1000 m or more apart), it is possible to obtain transmitters that can source up to 30,000 watts. Current is usually injected as a 50% duty cycle reversing square wave. That is, current is on for several seconds, off for several seconds, on with reversed polarity, off, etc. Voltages are recorded while current is on. This pattern for the current source is necessary because a voltage measured when the current is off will be non-zero in many situations. Naturally occuring potentials are called spontaneous or self-potentials (SP), and they are usually caused by electrochemical activity in the ground. From the point of view of DC resistivity surveys, SP voltages are noise because measured voltages must be caused by the source current only. The 50% duty cycle reversing square wave is employed so as to remove the (poorly known) SP signals.

2.3.2 Measurements

Potential difference it is tempting to compare the earth to a resistor in an electric circuit. However, it is important to recognize the difference between resistance and resistivity. If we apply Ohm's law, $R = \frac{V}{I}$, to the situation, we will have a resistance, which is in units of Ohms. This is NOT the ground's resistivity, which has units of Ohm-m. We do not want the resistance of this circuit; we want a measure of the ground's resistance per unit volume, or resistivity.

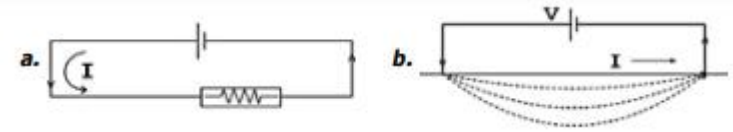

Figure 2.2: Relationship between current, voltage and resistance

In order to derive the relation between measurments (I, V, geometry) and the required physical property (resistivity). The actual measurement configuration can be summarized in the fig below;

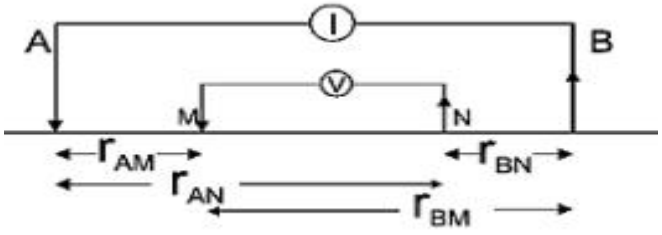

Figure 2.3: The measured voltage is a potential difference (VM - VN) in which each potential is the superposition of the effects from both current sources.

From the symmetry of the system shown in the diagram above, the potential will be a function of *r* only, where *r* is the distance from the first electrode. Under these

conditions Laplace's equation, in spherical coordinates, simplifies from equation 2.15 to equation 2.16.

$$\frac{\partial^2 V}{\partial r^2} + \frac{2\partial V}{r\partial r} + \frac{1}{r^2 sin\theta}\frac{\partial}{\partial \theta}\left(sin\theta \frac{\partial r}{\partial \theta}\right) + \frac{1}{r^2 sin^2\theta}\frac{\partial^2 V}{\partial \theta^2} = 0 \qquad (2.0)$$

$$\frac{d^2 V}{dr^2} + \frac{2}{r}\frac{dV}{dr} = 0 \qquad (2.1)$$

Multiplying by r^2, we get

$$r^2 \frac{d^2 V}{dr^2} + 2r\frac{dV}{dr} = 0$$

Which can be split as

$$r^2 \frac{d^2 V}{dr^2} = 0,\ 2r\frac{dV}{dr} = 0$$

Using the first of the two equations and neglecting the second because neither of its terms nor their product can be equal to zero, we have

$$r^2 \frac{d^2 V}{dr^2} = \frac{d}{dr}\left(r^2 \frac{dV}{dr}\right) = 0$$

Integrating,

$$\int \frac{d}{dr}\left(r^2 \frac{dV}{dr}\right) = \int 0$$

Which is $\frac{dV}{dr} = A$ or $\frac{dV}{dr} = \frac{A}{r^2}$ (2.2)

where A is a constant

Hence, $$dV = \frac{A}{r^2}dr \quad \text{and} \quad \int dV = \int \frac{A}{r^2}dr$$

$$V = -\frac{A}{r} + \mathrm{B} \qquad (2.3)$$

where A and B are constants. Because $V = 0$ when $r \to \infty$, we get $B = 0$. In addition, the current flows radially outward in all directions from the point electrode. Thus the total current crossing a spherical surface is given by

$$I = 4\pi r^2 J$$

but from equation (2.2), $J = \sigma E = -\sigma\, {dV}/{dr}$ since $E = -{dV}/{dr}$

$$I = -4\pi\sigma r^2\, {dV}/{dr}$$

Invoking equation (2.3)gives $I = -4\pi\sigma r^2\, {A}/{r^2} = -4\pi\sigma A$.

So that $A = -\frac{I}{4\pi\sigma}$. Therefore,

$$V = \frac{I}{4\pi\sigma r} = \frac{\rho I}{4\pi r} \quad \text{or} \quad \rho = \frac{4\pi r V}{I}$$

However, all the current flow through a hemispherical surface in the lower medium, hence,

$$A = -\frac{I}{2\pi\sigma}. \text{ Therefore,}$$

$$V = \frac{I}{2\pi\sigma r} = \frac{\rho I}{2\pi r} \quad \text{or} \quad \rho = \frac{2\pi r V}{I} \qquad (2.4)$$

For a current source and sink, the potential V_P at any point P in the ground is equal to the sum of the voltages from the two electrodes, such that: $V_P = V_A + V_B$ where V_A and V_B are the potential contributions from the two electrodes, A(+I) and B(- I). The potentials at electrode M and N are:

$$V_M = \frac{\rho I}{2\pi}\left[\frac{1}{AM} - \frac{1}{MB}\right], \; V_M = \frac{\rho I}{2\pi}\left[\frac{1}{AN} - \frac{1}{NB}\right]$$

Hence the potential difference between the two potential electrodes at points M and N can be written as:

$$\Delta V = V_M - V_N = \frac{\rho I}{2\pi}\left\{\left[\frac{1}{AM} - \frac{1}{MB}\right] - \left[\frac{1}{AN} - \frac{1}{NB}\right]\right\}$$

$$\rho = \frac{2\pi\Delta V}{I}\left\{\left[\frac{1}{AM} - \frac{1}{MB}\right] - \left[\frac{1}{AN} - \frac{1}{NB}\right]\right\}^{-1} \qquad (2.5)$$

The final expression in equation (2.5) is that for apparent resistivity. It has two parts, namely a resistance term *(*$R{=}\Delta V/I$*;* unit Ω) and a term that describes the geometry of the electrode configuration being used and which is known as the geometric factor *(K;* unit m).

$$\text{where } K = 2\pi\left\{\left[\frac{1}{AM} - \frac{1}{MB}\right] - \left[\frac{1}{AN} - \frac{1}{NB}\right]\right\}^{-1} \qquad (2.6)$$

Where *AM, AN, BM,* and *BN* are the distances between the current electrodes, *A* and *B,* and the potential electrodes, *M* and *N* as shown in the *Figure 2.2* above.

In electrical sounding using bipole-dipole or dipole-dipole arrays, *AM* nearly equals *AN* and *BM* nearly equals *BN;* therefore the calculation of ρ from the above equation requires the measurement of *AM, AN, BM,* and *BN* with great accuracy. Furthermore, by expressing the distances *AM, AN, BM,* and *BN* in terms of quantities *(AB, MN, R,* and θ) that are readily measured in the field, the expression of the geometric factor using the above equation becomes very complicated for nonlinear bipole-dipole arrays. To simplify the commutation of the geometric factor of bipole-dipole arrays, the apparent resistivity is expressed in terms of the electric field, *E,* instead of the potential difference,ΔV, and then the approximation $E = \Delta V/MN$ is used.

2.4 EXPRESSION FOR THE GEOMETRIC FACTOR (K)

Geometric factor (K_g) is a numerical multiplier defined by the geometrical spacing between electrodes, which is used in conjunction with the voltage-to-current (R) ratio measured in electrical resistivity surveys to give an apparent resistivity (ρ_a) such that $\rho a = Kg \times R$.

Mathematically;

(2.7)

$$\Delta V = \frac{I\rho}{2\pi}\left\{\frac{1}{r_{AM}} - \frac{1}{r_{BM}} - \frac{1}{r_{AN}} + \frac{1}{r_{BN}}\right\}$$

$$\Delta V = I\rho G$$

G is a geometric factor (including the factor $1/2\pi$), which depends upon the locations of electrodes.

2.4.1 Apparent resistivity

We are finally in a position to express the thing we want (a physical property) in terms of parameters we either know or measure (current, voltage and geometry). Rearranging the last expression above, we can define apparent resistivity as the halfspace resistivity which produces the observed potential from a particular electrode geometry:

$$\rho_a = \frac{\Delta V}{IG} \cdot \tag{2.8}$$

Similarly the apparent conductivity is

$$\sigma_a = \frac{1}{\rho_a} = \frac{IG}{\Delta V} \cdot \tag{2.9}$$

Apparent resistivity is the resistivity derived using only the known current, measured voltage, and array geometry. It is the earth's true resistivity only when the earth (within range of the measurements) is a uniform half space. When the earth is more complicated, the measured apparent resistivity will be less than the maximum and more than the minimum true (or intrinsic) resistivities that are within range.

2.4.2 The essence of interpreting resistivity surveys is to find the true distribution of intrinsic resistivities by interpreting the pattern of apparent resistivities that were measured.

Now we can find simple relations between all our known and measured quantities and a useful physical property, namely the apparent resistivity. We only need expressions for the geometric factor based upon electrode geometry. G is easily found if the four distances take on convenient values. For example, if electrodes are spaced equally by a distance a, then, using the figure and relation for V above,

$$G = (1/a - 1/2a - 1/2a + 1/a)/2 = 1/2a$$

This is the case for the "Wenner" array shown in Figure 2.3, which summarizes the geometric factor for a variety of common electrode configurations. Note that in this figure, k=1/G.

2.4.3 Anisotropic ground

Structural anisotropy (for example, layering or fracturing) causes the simple form of Ohm's law to break down because current flow is not necessarily parallel to the forcing electric field. Instead of simply writing as $= \sigma E = -\sigma \Delta V$, we have to write

$$J_i = -\sigma_{ik} \frac{\partial V}{\partial x_k} \quad i,k = 1,2,3.$$

In homogeneous ground with single current and potential electrodes, the expression for V (voltage) in terms of resistivity and distance from the current source is V= $I\rho/2\pi r$ (which was shown above). In anisotropic ground, there are different values of resistivity for the horizontal and a vertical direction. The

expression for voltage in terms of the two resistivities and distance is V $=-$ I$\rho_h\lambda/2\pi r$ where $\lambda = (\rho/\rho_h)^{1/2}$ is called the coefficient of anisotropy. See the table below for some values of λ encountered in common geological materials.

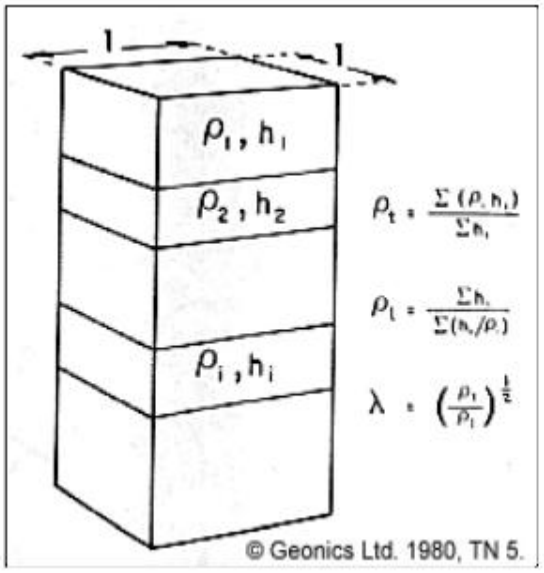

Rock type	Coefficient of anisotropy
Volcanic tuff, Eocene and younger, from Nevada	1.10–1.20
Alluvium, thick sections from the southwestern United States	1.02–1.10
Interbedded limestones and limey shales from northeastern Colorado	2.0 –3.0
Interbedded anhydrite and shale, northeastern Colorado	4.0 –7.5
Massive shale beds	1.01–1.05
Interbedded shale and sandstone	1.05–1.15
Baked shale or low-rank slate	1.10–1.60
Slates	1.40–2.25
Bitumenous coal and mudstone	1.7 –2.6
Anthracite coal and associated rocks	2.0 –2.6
Graphitic slate	2.0 –2.8

Figure 2.4: Coefficient for Anisotropic for layered rock (after Keller and Frichknechk)

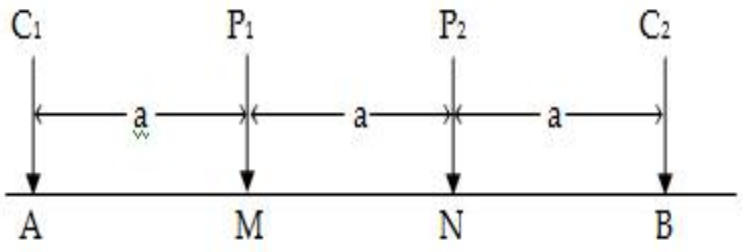

Figure 2.5: A Schematic of the electrode array configuration when using the Wenner array

Recalling Equation (2.6),

$$K = 2\pi\left\{\left[\frac{1}{AM} - \frac{1}{MB}\right] - \left[\frac{1}{AN} - \frac{1}{NB}\right]\right\}^{-1}$$

Where *AM, AN, BM,* and *BN* are the distances between the current electrodes, *A* and *B,* and the potential electrodes, *M* and *N* as shown in the figure above. From the diagram, $AM = NB = a$ and $AN = MB = 2a$. Therefore, Equation 2.11 becomes

$$K = 2\pi\left\{\left[\frac{1}{a} - \frac{1}{2a}\right] - \left[\frac{1}{2a} - \frac{1}{a}\right]\right\}^{-1} = 2\pi\left[\frac{1}{a} + \frac{1}{a} - \frac{1}{2a} - \frac{1}{2a}\right]^{-1}$$

$$= 2\pi\left[\frac{2}{a} - \frac{1}{a}\right]^{-1} = 2\pi\left[\frac{2-1}{a}\right]^{-1} = 2\pi a$$

Therefore the geometric factor for the Wenner array configuration is given by the expression $K = 2\pi a$. It is easy to show that when an "n" factor is included, to increase the electrode spacing for deeper current penetration, the K factor becomes $K = 2\pi an$.

2.4.4 Geometric Factor for Wenner-Schlumberger Array

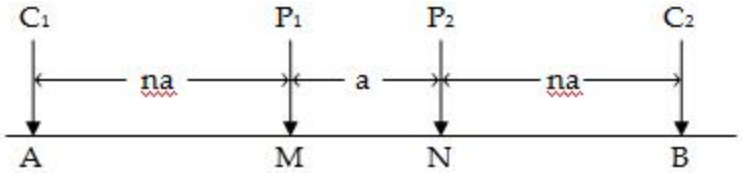

Figure 2.6: A Schematic of the Wenner-Schlumberger array electrode configuration

Recalling Equation(2.6),

$$K = 2\pi\left\{\left[\frac{1}{AM} - \frac{1}{MB}\right] - \left[\frac{1}{AN} - \frac{1}{NB}\right]\right\}^{-1}$$

Where *AM, AN, BM,* and *BN* are the distances between the current electrodes, *A* and *B,* and the potential electrodes, *M* and *N* as shown in the figure above. From the diagram, $AM = NB = an$ and $AN = MB = an + a = a(n+1)$. Therefore, Equation 2.7 becomes

$$K = 2\pi\left\{\left[\frac{1}{an} - \frac{1}{a(n+1)}\right] - \left[\frac{1}{a(n+1)} - \frac{1}{an}\right]\right\}^{-1}$$

$$= 2\pi\left[\frac{1}{an} + \frac{1}{an} - \frac{1}{a(n+1)} - \frac{1}{a(n+1)}\right]^{-1}$$

$$= 2\pi\left[\frac{2}{an} - \frac{2}{a(n+1)}\right]^{-1} = 2\pi\left[\frac{2(n+1) - 2n}{an(n+1)}\right]^{-1}$$

$$= 2\pi\left[\frac{2}{an(n+1)}\right]^{-1} = \pi an(n+1)$$

Therefore the geometric factor for the Wenner-Schlumberger array configuration is given by the expression$K = \pi an(n+1)$. It is worthy of note that the conventional Wenner array (Wenner Alpha) is actually a special case of the Wenner-Schlumberger array where the n factor is equal to 1. This array effectively becomes the Schlumberger array when the n factor is greater than 2. Thus the Wenner-Schlumberger array is actually a combination of the Wenner and Schlumberger

array adapted for use for an arrangement with a line of electrodes with a constant spacing (as normally used in 2-D electrical imaging).

2.4.5 Geometric Factor for Inline Dipole-dipole Array

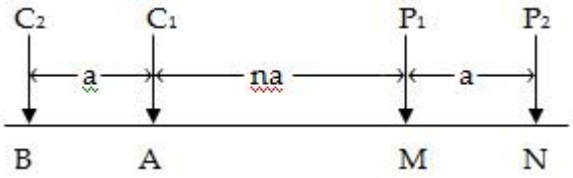

Figure 2.7: A Schematic of the electrode array configuration when using the Inline Dipole-dipole array

Recalling Equation 2.7,

$$K = 2\pi\left\{\left[\frac{1}{AM} - \frac{1}{MB}\right] - \left[\frac{1}{AN} - \frac{1}{NB}\right]\right\}^{-1}$$

Where *AM, AN, BM,* and *BN* are the distances between the current electrodes, *A* and *B,* and the potential electrodes, *M* and *N* as shown in the figure above. From the diagram, $AM = na$ and $AN = MB = na + a = a(n+1)$ and $NB = na + 2a = a(n+2)$. Therefore, Equation (2.7) becomes

$$K = 2\pi\left\{\left[\frac{1}{an} - \frac{1}{a(n+1)}\right] - \left[\frac{1}{a(n+1)} - \frac{1}{a(n+2)}\right]\right\}^{-1}$$

$$= 2\pi\left[\frac{1}{an} - \frac{2}{a(n+1)} + \frac{1}{a(n+2)}\right]^{-1}$$

$$= 2\pi\left[\frac{(n+1)(n+2)-2n(n+2)+n(n+1)}{an(n+1)(n+2)}\right]^{-1}$$

$$= 2\pi\left[\frac{n^2+3n+2-2n^2-4n+n^2+n}{an(n+1)(n+2)}\right]^{-1}$$

$$= 2\pi\left[\frac{2}{an(n+1)(n+2)}\right]^{-1} = \pi an(n+1)(n+2)$$

Therefore the geometric factor for the Inline Dipole-dipole array configuration is given by the expression $K = \pi an(n+1)(n+2)$.

2.4.6 Geometric Factor for Equatorial Dipole-dipole Array

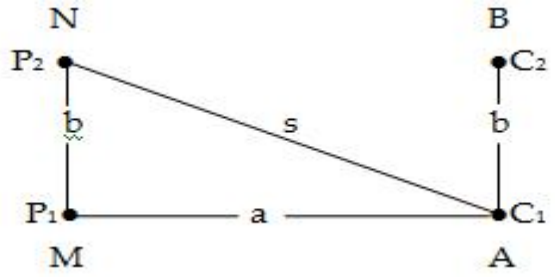

Figure 2.8: A Schematic of the electrode array configuration when using the Equatorial Dipole-dipole array

In this array, the electrode configuration is not symmetric. Hence Equation (2.6) becomes

$$K = 4\pi\left\{\left[\frac{1}{AM} - \frac{1}{MB}\right] - \left[\frac{1}{AN} - \frac{1}{NB}\right]\right\}^{-1}$$

Where *AM, AN, BM,* and *BN* are the distances between the current electrodes, *A* and *B,* and the potential electrodes, *M* and *N* as shown in the figure above. From the diagram,

$AM = NB = a$ and $MB = AN = s$, where using Pythagoras theorem,

$$s^2 = a^2 + b^2 \quad \therefore s = \sqrt{a^2 + b^2}$$

Using Equation(2.7) ,

$$K = 4\pi\left\{\left[\frac{1}{AM} - \frac{1}{MB}\right] - \left[\frac{1}{AN} - \frac{1}{NB}\right]\right\}^{-1} = 4\pi\left\{\left[\frac{1}{a} - \frac{1}{s}\right] - \left[\frac{1}{s} - \frac{1}{a}\right]\right\}^{-1}$$

$$= 4\pi\left[\frac{2}{a} - \frac{2}{s}\right]^{-1} = 4\pi\left[\frac{2s - 2a}{as}\right]^{-1}$$

$$= 4\pi\left[\frac{as}{2(s-a)}\right] = \frac{2\pi as}{s-a} \text{ where } \mathrm{s} = \sqrt{\mathrm{a}^2 - \mathrm{b}^2}$$

Therefore, the geometric factor for the Equatorial Dipole-dipole array electrode configuration is given by the expression

$$K = \frac{2\pi as}{s-a} \text{ where } \mathrm{s} = \sqrt{\mathrm{a}^2 - \mathrm{b}^2}$$

CHAPTER THREE

METHODOLOGY

3.1 FIELD SURVEY METHOD - MEASUREMENT PROCEDURE

Two-dimensional electrical imaging/tomography surveys are usually carried out using a large number of electrodes, 25 or more, connected to a multi-core cable (Griffiths and Barker, 1993). A laptop microcomputer together with an electronic

switching unit is used to automatically select the relevant four electrodes for each measurement (Figure 3.0). At present, field techniques and equipment to carry out 2-D resistivity surveys are fairly well developed. The necessary field equipment is commercially available from a number of international companies. Some institutions have even constructed “home-made” manually operated switching units at a nominal cost by using a seismic cable as the multi-core cable. Figure 3.1 shows the typical setup for a 2-D survey with a number of electrodes along a straight line attached to a multi-core cable. Normally a constant spacing between adjacent electrodes is used.

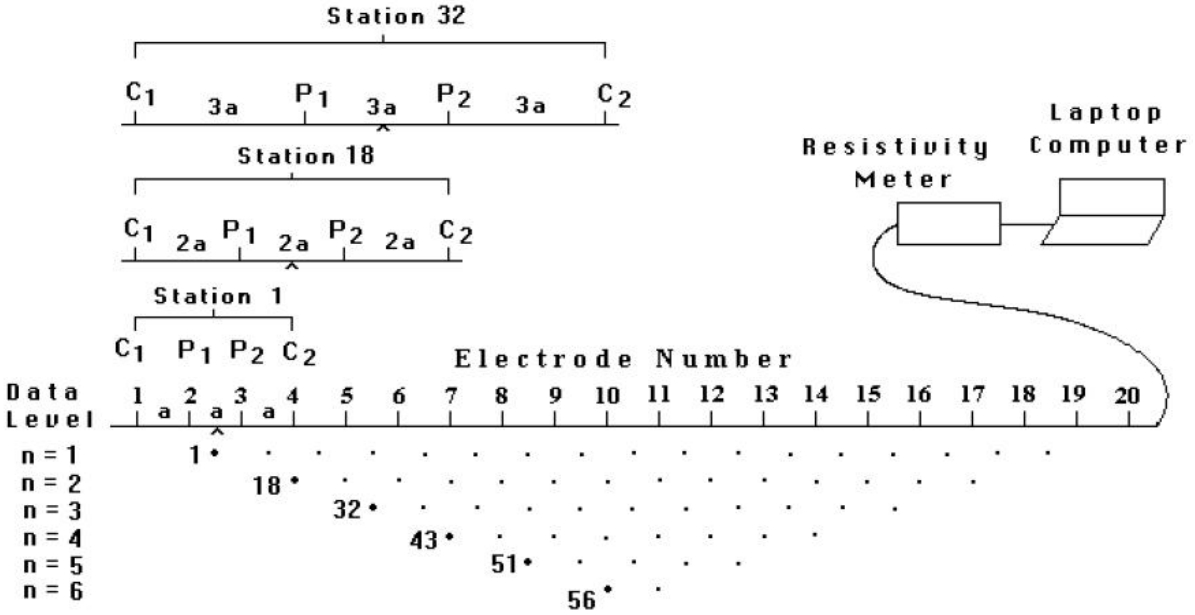

Figure 3.1: The arrangement of electrodes for a 2-D electrical survey using Wenner array and the sequence of measurements used to build up a pseudo section.

The multi-core cable is attached to an electronic switching unit that is connected to a laptop computer. The sequence of measurements to take, the type of array to use and other survey parameters (such as the current to use) is normally entered into a text file which can be read by a computer program in a laptop computer. Different resistivity meters use different formats for the control file, so one will need to refer to the manual for ones system. After reading the control file, the computer program then automatically selects the appropriate electrodes for each measurement. Some field systems have an in-built microprocessor system so that a laptop computer is not needed. This could be a significant advantage for surveys in very rugged terrain.

In a typical survey, most of the fieldwork is in laying out the cable and electrodes. After that, the measurements are taken automatically and stored in the computer. Most of the survey time is spent waiting for the resistivity meter to complete the set of measurements. To obtain a good 2-D picture of the subsurface, the coverage of the measurements must be 2-D as well.

Figure 3.1 shows a possible sequence of measurements for the Wenner electrode array for a system with 20 electrodes. In this example, the spacing between

adjacent electrodes is “a”. The first step is to make all the possible measurements with the Wenner array with electrode spacing of “1a”. For the first measurement, electrodes number 1, 2, 3 and 4 are used. Electrode 1 is used as the first current electrode C_1, electrode 2 as the first potential electrode P_1, electrode 3 as the second potential electrode P_2 and electrode 4 as the second current electrode C_2. For the second measurement, electrodes number 2, 3, 4 and 5 are used for C_1, P_1, P_2 and C_2 respectively. This is repeated down the line of electrodes until electrodes 17, 18, 19 and 20 are used for the last measurement with “1a” spacing. For a system with 20 electrodes, there are 17 i.e. (20 - 3) possible measurements with “1a” spacing for the Wenner array.

After completing the sequence of measurements with “1a” spacing, the next sequence of measurements with “2a” electrode spacing is made. First electrodes 1, 3, 5 and 7 are used for the first measurement. The electrodes are chosen so that the spacing between adjacent electrodes is “2a”. For the second measurement, electrodes 2, 4, 6 and 8 are used. This process is repeated down the line until electrodes 14, 16, 18 and 20 are used for the last measurement with spacing “2a”. For a system with 20 electrodes, there are 14 (20 - 2x3) possible measurements with “2a” spacing. The same process is repeated for measurements with “3a”, “4a”, “5a” and “6a”spacings. To get the best results, the measurements in a field survey should be carried out in a systematic manner so that, as far as possible, all the

possible measurements are made. This will affect the quality of the interpretation model obtained from the inversion of the apparent resistivity measurements (Dahlin and Loke, 1998).

As the electrode spacing increases, the number of measurements decreases. The number of measurements that can be obtained for each electrode spacing for a given number of electrodes along the survey line depends on the type of array used. The Wenner array gives the smallest number of possible measurements compared to the other common arrays that are used in 2-D surveys. The survey procedure with the pole-pole array is similar to that used for the Wenner array. For a system with 20 electrodes, firstly 19 of measurements with a spacing of "1a" are made, followed by 18 measurements with "2a" spacing, followed by 17 measurements with "3a" spacing, and so on.

For the dipole-dipole, Wenner-Schlumberger and pole-dipole arrays, the survey procedure is slightly different. As an example, for the dipole-dipole array, the measurement usually starts with a spacing of "1a" between the C_1-C_2 (and also the P_1-P_2) electrodes. The first sequence of measurements is made with a value of 1 for the "n" factor (which is the ratio of the distance between the C_1-P_1 electrodes to the C_1-C_2 dipole length), followed by "n" equals to 2 while keeping the C_1-C_2 dipole pair spacing fixed at "1a". When "n" is equals to 2, the distance of the C_1 electrode from the P_1 electrode is twice the C_1-C_2 dipole length. For subsequent

measurements, the “n” spacing factor is usually increased to a maximum value of about 6, after which accurate measurements of the potential are difficult due to very low potential values. To increase the depth of investigation, the spacing between the C_1-C_2 dipole pair is increased to “2a”, and another series of measurements with different values of “n” is made. If necessary, this can be repeated with larger values of the spacing of the C_1-C_2 (and P_1-P_2) dipole pairs. A similar survey technique can be used for the Wenner- Schlumberger and pole-dipole arrays where different combinations of the “a” spacing and “n” factor can be used.

For the parallel equatorial dipole-dipole array, the distance between the two current arrays are kept constant, say at “a” while the distance between the current electrode pair and the potential electrode pair, say “b” is varied. For example, the value of “a” could keep constant at 10meters while “b” varied from 10m to 20m, 30m and so on. This is the method applied in this work.

One technique used which can be used (but was not used for this work) to extend horizontally the area covered by the survey, particularly for a system with a limited number of electrodes, is the roll-along method. After completing the sequence of measurements, the cable is moved past one end of the line by several unit electrode spacings. All the measurements that involve the electrodes on part of the cable that do not overlap the original end of the survey line are repeated (Figure 3.1). This

technique is similar to offset – Wenner method used in 1-D electrical resistivity surveying.

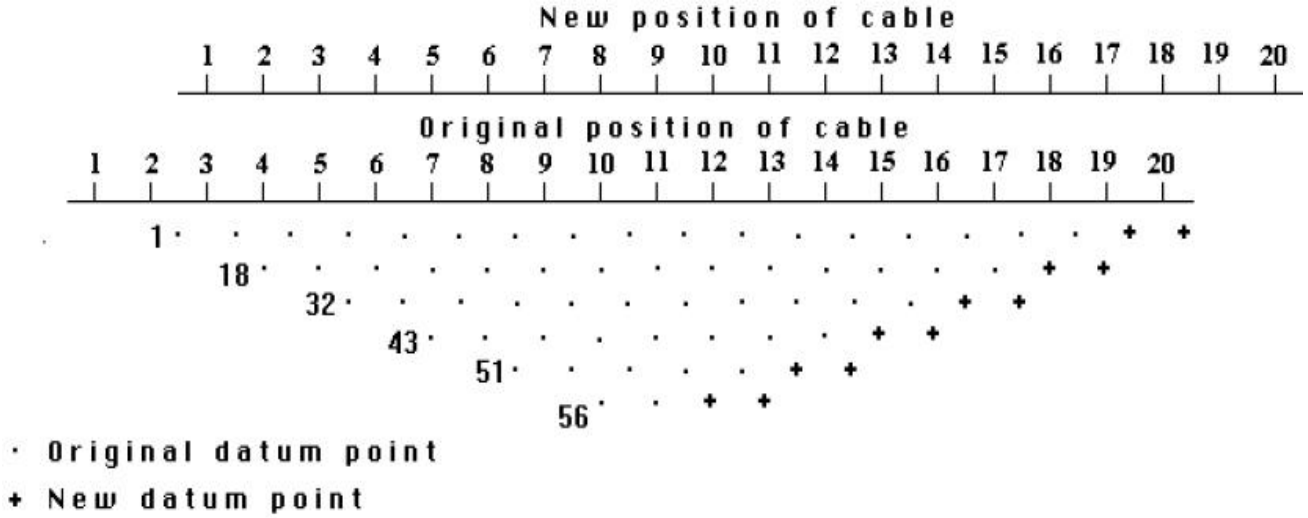

Figure 3.2: The use of the roll-along method to extend the area covered by a 2-D survey.

3.2 CLASSIFICATION OF ELECTRICAL RESISTIVITY MEASURING INSTRUMENTS (TERRAMETERS)

The instrument type can be divided into two broad categories: static and dynamic systems. Most instruments are of the static type where many electrodes are connected to a multi-electrode cable and planted into the ground during the survey. A typical static system is the Abem Lund system. One common configuration is a

split spread type of cable connect-ion to the switching unit at the center to reduce the individual cable length and weight. The weight of a cable roll is directly proportional to the number of nodes and the spacing between the nodes. A common spacing used for most engineering and environmental surveys is 5 meters. Most systems come with a minimum of 28 nodes, with some system having up to 128 nodes or more. The Lund system is a little unusual in that there are 4 individual cables. Most systems use a 2 cables arrangement. The static systems can be further divided into two sub-categories depending on the arrangement for the switching of the electrodes. Most of the systems house the switches in a single unit and uses a cable with many individual wires connected to each node. Typical examples are the Abem Lund and Campus Geopulse systems. Another arrangement is to have a small switching unit at each electrode and a cable with the minimum number of wires. One early example is the Campus MRT system (Griffiths and Turnbull, 1985). A more recent example is the PASI system.

There have been two new and interesting developments in the resistivity meter systems. One is the addition of I.P. capability. The second is multi-channel measuring systems. In such a system, a number of potential measurements can be simultaneously made for a single pair of current electrodes. This could significantly reduce the survey time. With certain array configurations, a single 2-D survey line could involve thousands of measurements. The major part of the

survey time is waiting for a single channel instrument to complete the measurements that could take more than several hours.

Static systems use a large number of nodes to get a wide data coverage. In contrast, dynamic systems use a small number of nodes but move the entire system to obtain a wide coverage. An example of such a system is that designed by Aarhus University in Denmark (Sorenson 1996). It uses a 100 meters cable with nine heavy cylindrical electrodes pulled by a small vehicle. Two of the electrodes are used as current electrodes, while six of them are used for the potential measurements and one is used as a ground electrode. This system relies on the current being injected into the ground by direct contact, so it can only be used in open ground, such as farmlands. A Wenner-Schlumberger type of arrangement is used but with non-integer "n" values for some of the measurements. Another mobile system that does not require direct contact with the ground but uses capacitive coupling to induce the flow of current in the ground is the Geometrics Ohm Mapper system where a cable with 4 to 6 electrodes attached to a measuring unit is pulled by a single operator (Gerard and Tabbagh, 1991; Shima et al., 1996; Panissod et al., 1998). This system can be used in areas that are paved, such as roads and city areas. Since the capacitive coupling type does not require direct ground contact, it can be used in many areas where normal resistivity surveying systems cannot be used (for example in built-up areas). It however has the problem

of a more limited depth of penetration due to the limited amount of current that can be induced into the ground compared to direct contact systems. An underwater environment provides an almost ideal situation for a direct contact type of mobile system since there is no problem in obtaining good electrode contact. For an underwater mobile surveying system where a cable with a number of nodes is pulled along the river/lake/sea bottom by a boat, two of the nodes are used as current electrodes, while the rest are used as potential electrodes. If this system is coupled with a multi-channel resistivity meter, the survey can be carried out very rapidly. Shallow seismic reflection surveys are frequently used in rivers/lakes/marine environments for engineering site surveys. A mobile resistivity survey might be a useful addition in some situations, such as in seismically opaque areas. In theory, both surveys can be carried out simultaneously to reduce costs. Other field instrument include the following;

1. Measuring Tape: This is used to measure the length of spread of both the potential and current electrodes. It is calibrated in centimeter, meter and feet. In cases where the length of the spread is exhausted and there are still distances to be measured, measured distances on the ground can be marked and the remainder of the distance, measured.

2. Electrodes: These are metallic conductors used in field work because of their high conductivity. One end of the metal is pointed; this is to ease its penetration into the ground.

3. Current and Potential Electrode Cables: These are made of electrical cables which are wound around insulators which can be rolled. On the field, one end of the cable is reeled out and used to make contact with the electrodes. Current is sent from an electrical power source, through the cable, to the current electrodes which then transmit this current into the earth. The cable is also used to connect both the current and potential electrodes to the terrameter.

4. Terrameter: This is a computerized system which is at the heart of the entire field operation. There are numerous, and these have been discussed analytically in the preceding section.

5. Hammer: This is used to hit the electrodes into the earth for greater penetration in areas of highly compacted soil structure.

6. Battery: This is used to power the terrameter. It is also the source of the current which is sent into the earth, from which the potential difference across the potential electrodes is measured.

7. Cutlass: This is used in rough terrain. It is used to clear off weeds, grasses and all unwanted obstruction along the walk-way or on points disturbing the placement of electrodes.

8. Geographical Positioning System (GPS): This is used to obtain knowledge of geographical location (longitude and latitude) of the survey area. It is very important, in that it tells us the elevation of the surface layer with respect to the sea level. This is needed for accurate analysis of the position of subsurface anomalies.

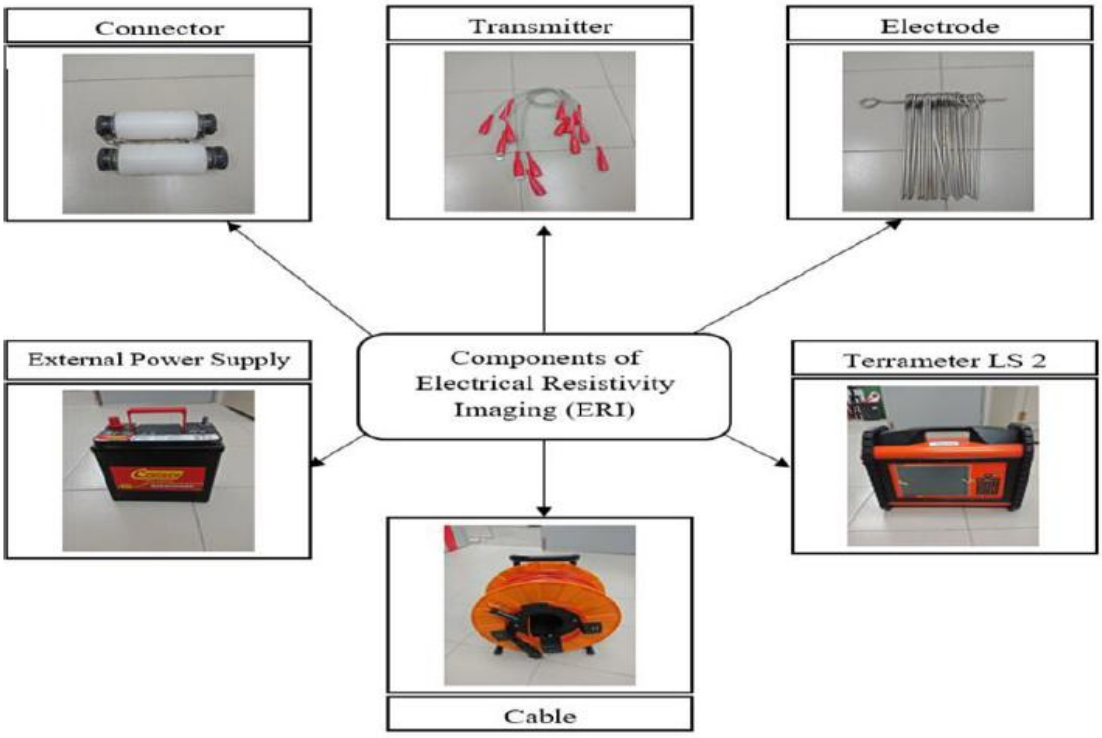

Figure 3.3: Basic field equipment for this research

3.3 PSEUDOSECTION DATA PLOTTING METHOD

To plot the data from a 2-D imaging survey, the pseudosection contouring method is normally used. In this case, the horizontal location of the point is placed at the mid-point of the set of electrodes used to make that measurement. The vertical location of the plotting point is placed at a distance that is proportional to the separation between the electrodes.

Another method is to place the vertical position of the plotting point at the median depth of investigation (Edwards, 1977), or pseudodepth, of the electrode array used. This pseudodepth value is based on the sensitivity values or Frechet derivative for a homogeneous half space. The pseudosection plot obtained by contouring the apparent resistivity values is a convenient means to display the data.

The pseudosection gives a very approximate picture of the true subsurface resistivity distribution. However the pseudosection gives a distorted picture of the subsurface because the shapes of the contours depend on the type of array used as well as the true subsurface resistivity. The pseudosection is useful as a means to present the measured apparent resistivity values in a pictorial form, and as an initial guide for further quantitative interpretation. One common mistake made is to try to use the pseudosection as a final picture of the true subsurface resistivity. Different arrays used to map the same region can give rise to very different contour shapes in the pseudosection plot. It is worthy to note that the pole-pole array gives the widest horizontal coverage, while the coverage obtained by the Wenner array

decreases much more rapidly with increasing electrode spacing. One useful practical application of the pseudosection plot is for picking out bad apparent resistivity measurements. Such bad measurements usually stand out as points with unusually high or low values.

3.4 HIGH-RESOLUTION ELECTRICAL SURVEYS WITH OVERLAPPING DATA LEVELS

In seismic reflection surveys, the common depth point method is frequently used to improve the quality of the signals from subsurface reflectors. A similar technique can be used to improve the data quality for resistivity/IP surveys, particularly in noisy areas. This is by using overlapping data levels with different combinations of "a" and "n" values for the Wenner-Schlumberger, dipole-dipole and pole-dipole arrays.

To simplify matters, let us consider the case for the Wenner-Schlumberger array with an inter-electrode spacing of 1 meter along the survey line. A high-resolution Wenner-Schlumberger survey will start with the "a" spacing (which is the distance between the P_1-P_2 potential dipole) equals to 1 meter and repeat the measurements with "n" values of 1, 2, 3 and 4. Next the "a" spacing is increased to 2 meter, and

measurements with “n” equals to 1, 2, 3 and 4 are made. This process is repeated for all possible values of the “a” spacing. To be on the safe side, the data set should contain all the possible data points for the Wenner array. The number of data points produced by such a survey is more than twice that obtained with a normal Wenner array survey. Thus the price of better horizontal data coverage and resolution is an increase in the field survey time.

A Wenner array with “a” equals to 2 meters will have a total array length of 6 meters. In comparison with the Wenner array, the Wenner-Schlumberger array will have a slightly smaller (approximately the same) depth of investigation. While the depth of investigation of the two arrangements are similar, the section of the subsurface mapped by the two arrays will be slightly different due to the different sensitivity patterns. So the two measurements will give slightly different information about the subsurface. If measurements obtained from three different values of “a” are used, the data set will have measurements with three different pseudodepths. This results in a pseudosection with overlapping data levels.

A similar “high-resolution” survey technique can also be used with the dipole-dipole and pole-dipole arrays by combining measurements with different “a” and “n” values to give overlapping data levels. In particular, this technique might be useful for the dipole-dipole array since the signal strength decreases rapidly with increasing "n" values. A typical high resolution dipole-dipole survey might use the

following arrangement; start with a dipole of "1a" and "n" values of 1, 2, 3, 4, 5; followed by a dipole of "2a" and "n" values of 1, 2, 3, 4, 5; and if necessary another series of measurements with a dipole of "3a" and "n" values of 1, 2, 3, 4, 5. Measurements with the higher "n" values of over 4 would have higher noise levels. However, by having such redundant measurements using the overlapping data levels, the effect of the more noisy data points will be reduced. This arrangement has been widely used for IP surveys with the dipole-dipole array (Edwards 1977).

In theory, it should be possible to combine measurements made with different arrays to take advantage of the different properties of the various arrays. Although this is not a common practice, it could conceivably give useful results in some situations.

3.5 FIELD PRECAUTIONS

1. Readings were not taken during thunder storms or beneath any overhead or high-tension cable because the high voltage flowing through them could be induced into the electrodes and as such alter the value of the potential measured. In the case of very high voltages, the induced current can be high enough to damage the terrameter.

2. The terrameter was protected from the heat of the sun because this could affect the internal resistance of the terrameter and hence the readings obtained as a result of the increase in temperature.

3. Care was taken not to unnecessarily stretch the wire as this could lead to an internal cut.

4. As much as possible, the current electrodes were maintained along a straight line relative to the positions of the potential electrodes, unless the array necessitated a different electrode spread.

5. Because of the closeness of the knobs which form part of the terrameter, caution was taken to avoid contact between the wires connecting the different electrodes as this could lead to erroneous readings from the terrameter and in serious cases, could even damage the terrameter.

6. As much as possible, contact between surface water and the electrodes was avoided during the field work so as to reduce wanted potentials and the accompanying unnecessary resistivity anomalies.

7. When current was sent from the terrameter, contact with the current electrodes was avoided because, when high current is used, it can lead to electrocution.

CHAPTER FOUR

RESULT AND DISCUSSION

4.1 RESULT

Table 4.1: 2-D Electrical Resistivity Field Record – Traverse seven

Date: 15-2-2021 **Instrument: PASI Earth resistivity Meter**

Location: Ogbogiobo, Ovia North East Local Government Area of Edo State

Geometric Factor, $K = 2\pi a$

Wenner traverse 7 Long 005˚38'42.52" Lat 06˚31'55.88" Elev 122m					
Traverse 7 a = 10m					
C1	P1	P2	C2	R(Ω)	ρ(Ωm)
0	10	20	30	29.1	1828.644
10	20	30	40	28.1	1765.804
20	30	40	50	16.8	1055.712

30	40	50	60	23.9	1501.876
40	50	60	70	28.5	1790.94
50	60	70	80	30.4	1910.336
60	70	80	90	31	1948.04
70	80	90	100	41.4	2601.576
80	90	100	110	39	2450.76
90	100	110	120	49.3	3098.012
100	110	120	130	48.3	3035.172
110	120	130	140	57.3	3600.732
120	130	140	150	45.1	2834.084
130	140	150	160	48.5	3047.74
140	150	160	170	52.7	3311.668
150	160	170	180	47	2953.48
160	170	180	190	52.9	3324.236
170	180	190	200	54.4	3418.496
Traverse 7 a = 20m					
C1	P1	P2	C2	R(Ω)	ρ(Ωm)
0	20	40	60	13.3	1671.544
10	30	50	70	11.2	1407.616
20	40	60	80	15.3	1922.904
30	50	70	90	16.3	2048.584
40	60	80	100	16.7	2098.856
50	70	90	110	20.7	2601.576
60	80	100	120	21.8	2739.824

70	90	110	130	17.8	2237.104
80	100	120	140	19.7	2475.896
90	110	130	150	24.2	3041.456
100	120	140	160	24.7	3104.296
110	130	150	170	20.6	2589.008
120	140	160	180	23.7	2978.616
130	150	170	190	22.1	2777.528
140	160	180	200	22.4	2815.232
Traverse 7 a = 30m					
C1	P1	P2	C2	R(Ω)	ρ(Ωm)
0	30	60	90	10	1885.200
10	40	70	100	12.4	2337.648
20	50	80	110	14.8	2790.096
30	60	90	120	16.1	3035.172
40	70	100	130	14.6	2752.392
50	80	110	140	14.4	2714.688
60	90	120	150	14.3	2695.836
70	100	130	160	15	2827.800
80	110	140	170	16.3	3072.876
90	120	150	180	16.6	3129.432
100	130	160	190	15.5	2922.060
110	140	170	200	15	2827.800
Traverse 7 a = 40m					
C1	P1	P2	C2	R(Ω)	ρ(Ωm)

0	40	80	120	12.3	3091.728
10	50	90	130	13.4	3368.224
20	60	100	140	12.8	3217.408
30	70	110	150	13.3	3343.088
40	80	120	160	13.1	3292.816
50	90	130	170	12.3	3091.728
60	100	140	180	13.5	3393.36
70	110	150	190	13.1	3292.816
80	120	160	200	12.7	3192.272
Traverse 7 a = 50m					
C1	P1	P2	C2	R(Ω)	ρ(Ωm)
0	50	100	150	11.8	3707.56
10	60	110	160	11.6	3644.72
20	70	120	170	11.8	3707.56
30	80	130	180	11.8	3707.56
40	90	140	190	10.5	3299.1
50	100	150	200	10.5	3299.1
Traverse 7 a = 60m					
C1	P1	P2	C2	R(Ω)	ρ(Ωm)
0	60	120	180	10.5	3958.92
10	70	130	190	10.5	3958.92
20	80	140	200	9.8	3694.992
Wenner traverse 7 Long 005˚38'42.52" Lat 06˚31'55.88" Elev 122m					

Table 4.2: 2-D Electrical Resistivity Field Record – Traverse eight

Date: 15-2-2021 **Instrument: PASI Earth resistivity Meter**

Location: Ogbogiobo, Ovia North East Local Government Area of Edo State

Geometric Factor, $K = 2\pi a$

Wenner traverse 8 Long 005˚38'43.75" Lat 06˚31'55.93" Elev 120m					
Traverse 8 a = 10m					
C1	P1	P2	C2	R(Ω)	ρ(Ωm)
0	10	20	30	32.4	2036.016
10	20	30	40	30.2	1897.768
20	30	40	50	28.4	1784.656
30	40	50	60	22.6	1420.184
40	50	60	70	36.8	2312.512
50	60	70	80	36.2	2274.808
60	70	80	90	42.2	2651.848
70	80	90	100	38.6	2425.624

80	90	100	110	40.2	2526.168
90	100	110	120	42.4	2664.416
100	110	120	130	38.6	2425.624
110	120	130	140	32.4	2036.016
120	130	140	150	35.4	2224.536
130	140	150	160	38.6	2425.624
140	150	160	170	42.4	2664.416
150	160	170	180	29.6	1860.064
160	170	180	190	30.4	1910.336
170	180	190	200	36.6	2299.944
Traverse 8 a = 20m					
C1	P1	P2	C2	R(Ω)	ρ(Ωm)
0	20	40	60	25.4	3192.272
10	30	50	70	19.4	2438.192
20	40	60	80	18.6	2337.648
30	50	70	90	19.6	2463.328
40	60	80	100	20.2	2538.736
50	70	90	110	19.4	2438.192
60	80	100	120	19.6	2463.328
70	90	110	130	22.4	2815.232
80	100	120	140	20.6	2589.008
90	110	130	150	19.6	2463.328
100	120	140	160	32.2	4046.896
110	130	150	170	23.6	2966.048

120	140	160	180	19.4	2438.192
130	150	170	190	19.4	2438.192
140	160	180	200	22.2	2790.096
Traverse 8 a = 30m					
C1	P1	P2	C2	R(Ω)	ρ(Ωm)
0	30	60	90	15.6	2940.912
10	40	70	100	14.2	2676.984
20	50	80	110	14.6	2752.392
30	60	90	120	15.2	2865.504
40	70	100	130	14.8	2790.096
50	80	110	140	14.2	2676.984
60	90	120	150	15.2	2865.504
70	100	130	160	14.1	2658.132
80	110	140	170	18.4	3468.768
90	120	150	180	15.6	2940.912
100	130	160	190	15.6	2940.912
110	140	170	200	14.1	2658.132
Traverse 8 a = 40m					
C1	P1	P2	C2	R(Ω)	ρ(Ωm)
0	40	80	120	11.6	2915.776
10	50	90	130	12.9	3242.544
20	60	100	140	13.2	3317.952
30	70	110	150	11.9	2991.184
40	80	120	160	12.2	3066.592

50	90	130	170	14.2	3569.312
60	100	140	180	13.2	3317.952
70	110	150	190	12.8	3217.408
80	120	160	200	12.4	3116.864
Traverse 8 a = 50m					
C1	P1	P2	C2	R(Ω)	ρ(Ωm)
0	50	100	150	11.2	3519.04
10	60	110	160	11.7	3676.14
20	70	120	170	11.7	3676.14
30	80	130	180	12.2	3833.24
40	90	140	190	11.8	3707.56
50	100	150	200	12.8	4021.76
Traverse 8 a = 60m					
C1	P1	P2	C2	R(Ω)	ρ(Ωm)
0	60	120	180	9.8	3694.992
10	70	130	190	10.6	3996.624
20	80	140	200	10.6	3996.624
Wenner traverse 8 Long 005˚38'45.20" Lat 06˚31'50.77" Elev 114m					

4.2 INTERPRETATION OF RESULTS

The resistivity of common rocks, soils and other materials, resistivity survey gives a picture of the subsurface resistivity distribution. To convert resistivity picture into a geological picture, some knowledge of typical resistivity values for different types of subsurface materials and the geology of the area surveyed, is important.

Table 4.3: Resistivity values of common rocks, soil materials and chemicals (Loke, 2000).

Material	Resistivity (Ωm)
Sandstone	$8 – 4 \times 10^3$
Shale	$20 – 2 \times 10^3$
Limestone	$50 – 4 \times 10^2$
Clay	1 - 100
Alluvium	10 - 800
Ground water (fresh)	10 - 100
Sea water	0.2
Ash	4
Colliery spoil	10 - 20
Pulverized fuel ash	50 - 100
Laterite	800 - 1500
Lateritic soil	120 - 750
Dry sandy soil	80 – 1050
Sand clay/ clayey sand	30 - 215
Sand and gravel	30 – 225
Unsaturated landfill	30 – 100
Saturated landfill	15 – 30
Acid mine water	20
Rainfall runoff	20 – 100
Landfill runoff	$< 10 – 50$

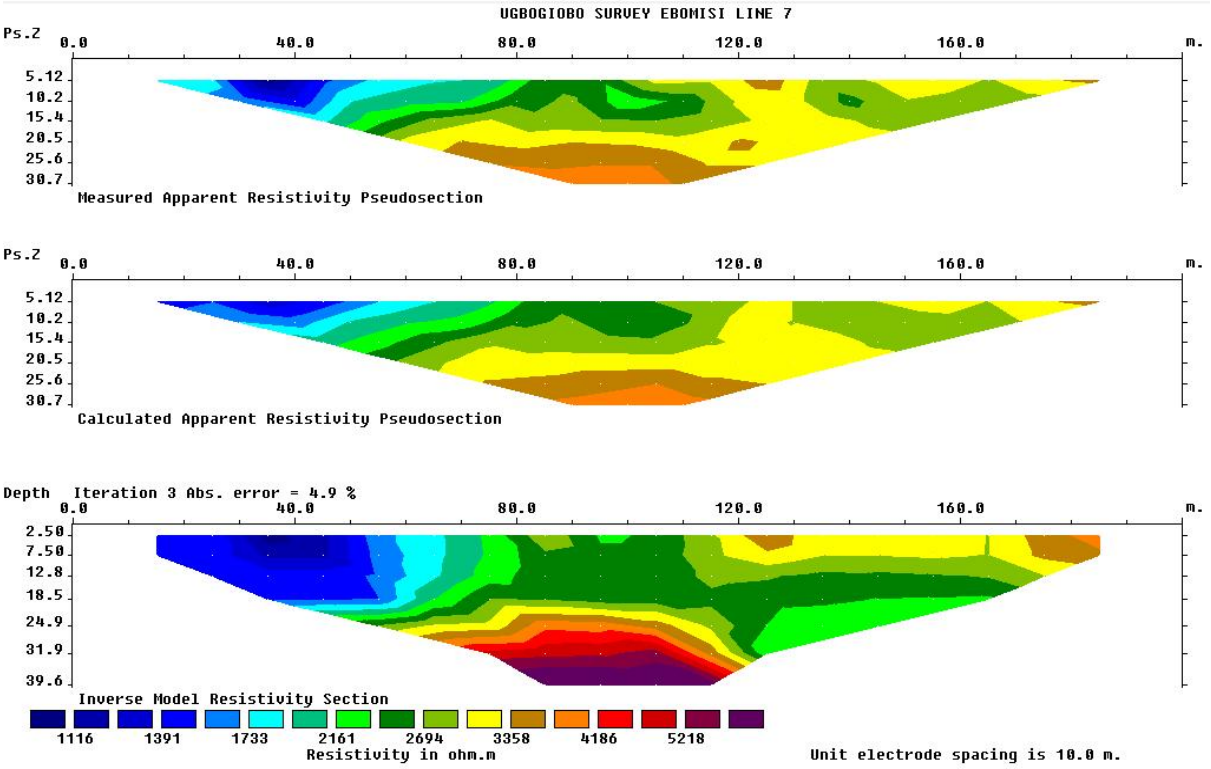

Figure 4.1: Inverted 2-D resistivity imaging model obtained from Ugbogiobo community profile seven.

Six (6) major resistivity structures were delineated in the profile which is seen to be generally characterized by moderate resistivity values, at the top layers we can inferred from the low resistivity that is characterize by Clayey and Alluvium soil having a resistivity range between 200 Ωm – 800 Ωm. The major mineral occurrence in this profile are majorly compose of sedimentary Rocks ranging from Limestone, Shale and Sandstone with a resistivity range for Limestone between 2000 Ωm – 3000 Ωm, Shale with a resistivity range 3200 Ωm – 4000 Ωm Sandstone between resistivity range 4000 Ωm – 5000 Ωm.

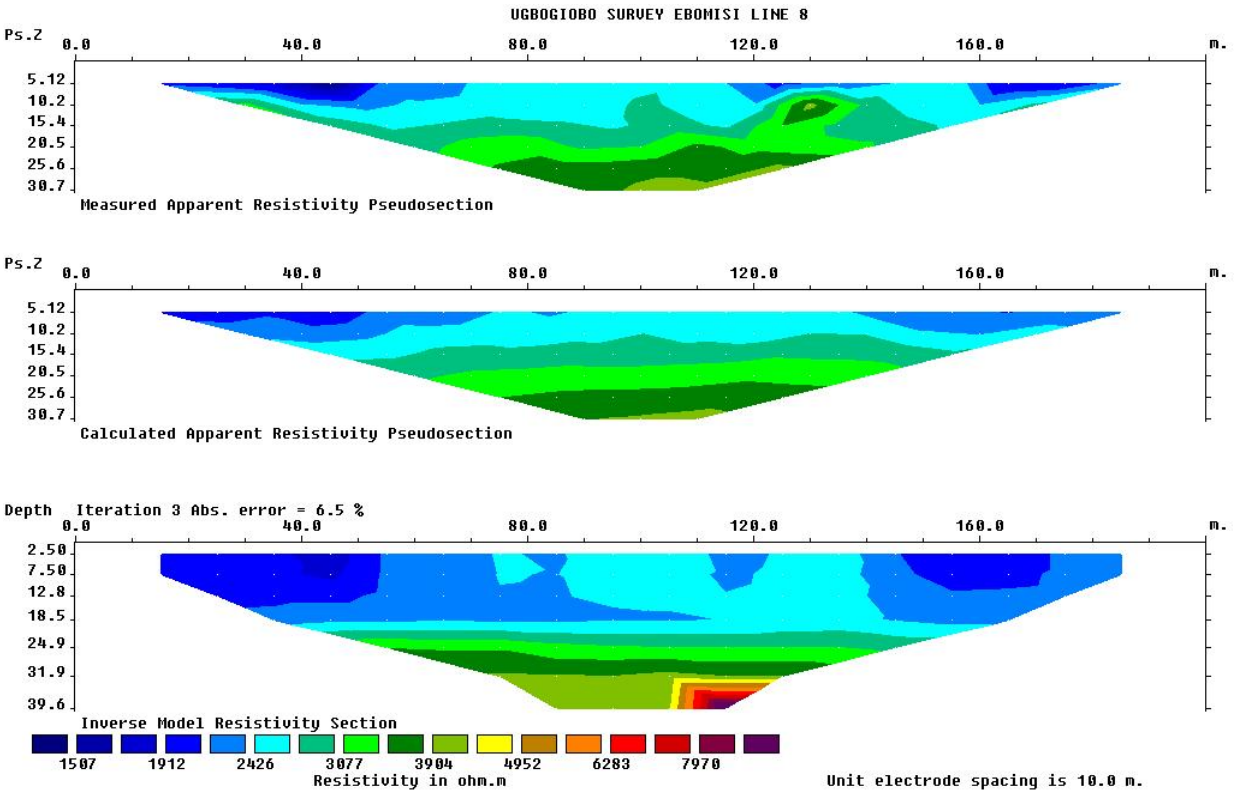

Figure 4.2: Inverted 2-D resistivity imaging model obtained from Ugbogiobo community profile eight

Five (5) major resistivity structures were delineated in the profile which is seen to be generally characterized by moderate resistivity values, the profile suggest the presence of sedimentary minerals. The major mineral occurrence in this profile are majorly compose of sedimentary Rocks ranging from Limestone, Shale and Sandstone with a resistivity range for Limestone between 2000 Ωm – 3000 Ωm, Shale with a resistivity range 3200 Ωm – 4000 Ωm Sandstone between resistivity range 4000 Ωm – 5000 Ωm and at the top layers we can inferred from the low resistivity that is characterize by Clayey and Alluvium soil having a resistivity

range between 200 Ωm – 800 Ωm, it will be noticed from the profiled line that all inferred mineral types fall between a depth of 2 m to 39 m. which form the lithological mineral occurrence of the profile.

Table: 4.4 Lithological Interpretation of the 2-D Data inversion

Resistivity(Ωm)	**Inferred Rock Type**	**DEPTH(m)**	**Standard Resistivity (Ω•m) values for rocks.**
500-1000	Limestone	25m	10^2 - 10^6
2000-8000	Quartz, Marble	30m	10^2 - $2x10^8$
1300-35000	Magnetite	35m	$5x10^{-3}$ -$5.7x10^3$
80000-300000	Stibnite	53m	10^5 - 10^{12}

CHAPTER FIVE

FINDINGS, CONCLUSION AND SUGGESTION FOR FURTHER STUDIES

5.1 FINDINGS

1. The results from the 2-D data survey, 2-D images of the subsurface Lithology of the study area was captured.

2. It is evident from the result obtained from the inverted 2D data, that the study area is characterize by the various mineral occurrences like Alluvium, Clayey soil, limestone, sandstone, clay.

5.2 CONCLUSION

2-D survey of a part of Ugbogiobo community and its environs has been carried out successfully and this research has helped in providing information about the subsurface of the study area. This information is of utmost importance as it gives the necessary constituents of the profile of the study area. The subsurface of a study area is related to various geological parameters such as mineral and fluid content, porosity and degree of water saturation in the rock.

2-D technique is a powerful tool to delineate sub-surface structure, when there is sufficient resistivity contrast. Nowadays two dimensional resistivity measurements

are quite easy, low-cost and fast to implement as new, advanced and fully automated resistivity instruments have been developed. Furthermore the development of two dimensional inversion resistivity algorithms has aided the processing and interpretation of complex data.

In summary, due to the inferred rock types and mineral occurences (Alluvium, Clayey soil, limestone, sandstone, and clay) gotten from the lithological interpretation of the 2-D data inversion, it can be concluded that the lithology of the study area is good for engineering purpose and construction work.

5.3 SUGGESTION FOR FURTHER STUDIES

1. More than one array system in more than one profile is always necessary before proper inference can be made in reference to structural lithology.
2. It is suggested that if any geophysical work is to be carried out anywhere near this same location, there should be a wider spread so as to achieve a deeper current penetration and consequently get a better image resolution in the interpretation and result.
3. More work should be done to enhance the efficiency of 2-dimensional electrical resistivity interpreting software, so that sharp contrasts in resistivity can be recorded.

REFERENCES

Aigbogun, C.O. (2010). Geolectric investigation of the groundwater potential in Uhunmwode Local Government Area, Edo State, Nigeria. Ph.D Thesis, University of Benin, Benin City, Edo State Nigeria.

Alile O.M, Amadasun C.V.O. and Evbuomwan A.L. (2008). Application of Vertical Electrical Sounding Method to Decipher the Existing Subsurface Stratification and Groundwater Occurrence Status in a Location in Edo North of Nigeria. Int. J. Phys. Sci., 3(10): 245–249.

Avbovbo, A. A. (1978). Tertiary lithostratigraphy of Niger Delta: American Association of Petroleum Geologists Bulletin, v. 62, p. 295-300.

Burke, K. (1972). Longshore drift, submarine canyons, and submarine fans in development of Niger Delta: American Association of Petroleum Geologists, v. 56, p. 1975-1983.

Doust, H., and Omatsola, E. (1990). Niger Delta, in, Edwards, J. D., and Santogrossi, P.A., Divergent/passive Margin Basins, AAPGMemoir 48: Tulsa, American Association of Petroleum Geologists, p.239-248.

Driscoll, F.G. (1986). Groundwater and Wells. 2nd edition, Johnson Division, St Paul,Minnesota, 1089 pp.

Evamy, B.D., Haremboure, J., Kamerling, P., Knaap, W.A., Molloy, F.A., and Rowlands, P.H. (1978). Hydrocarbon habitat of Tertiary Niger Delta: American Association of Petroleum Geologists Bulletin, v. 62, p. 277-298.

Freeze, R.A. and Cherry, J.A. (1979). Groundwater. Prentice-Hall, Englewood Cliffs, New Jersey, 604 pp.

Hospers, J. (1965). Gravity field and structure of the Niger Delta, Nigeria, West Africa: Geological Society of American Bulletin, v. 76, p. 407-422.

Kaplan, A., Lusser, C.U., Norton, I.O. (1994). Tectonic map of the world, panel 10: Tulsa, American Association of Petroleum Geologists, scale 1:10,000,000

Keller, G. V. and Frischknecht, F. C. (1966). Electrical methods in geophysical prospecting. Pergamo Press Inc., Oxford.

Klett, T.R., Ahlbrandt, T.S., Schmoker, J.W., and Dolton, J.L. (1997). Ranking of the world's oil and gas provinces by known petroleum volumes: U.S.Geological Survey Open-file Report-97-463, CD-ROM.

Koefoed, O.C. (1979). Geosounding Principles 1: Resistivity Sounding Measurements.ElsevierScience Publishing Company: Amsterdam, The Netherlands.

Kulke, H. (1995). Nigeria, in, Kulke, H.,ed., Regional Petroleum Geology of the World. Part II: Africa, America, Australia and Antarctica: Berlin, Gebrüder Borntraeger, p. 143-172.

Lehner, P., and De Ruiter, P.A.C. (1977). Structural history of Atlantic Margin of Africa: American Association of Petroleum Geologists Bulletin, v. 61, p. 961-981.

Loke M.H. (2000). Electrical imaging surveys for environmental and engineering studies. Available at http://www.geoelectrical.com

Nwachukwu, S.O. (1972). The tectonic evolution of the southern portion of the Benue Trough, Nigeria: Geology Magazine, v. 109, p. 411-419.

Reijers, T.J.A., Petters, S.W., and Nwajide, C.S. (1997). The Niger Delta Basin, in Selley, R.C.,eds., African Basins--Sedimentary Basin of the World 3: Amsterdam, Elsevier Science, pp. 151-172.

Reynolds,J.M. (1997). An Introduction to Applied and Environmental Geophysics.John Wiley and Sons Limited,West Sussex,England.

Reyment, R.A. (1965). Aspect of Geology of Nigeria. University of Ibadan Press.

Sch¨on, J. H. (1996). Physical properties of rocks: fundamentals and principles of petrophysics.Pergamo Press Inc., Oxford.

Shannon, P. M., and Naylor, N. (1989). Petroleum Basin Studies: London, Graham and Trotman Limited, p 153-169.

Sharma,V.P. (1999).Applied and environmental geophysics. Cambridge University Press, Cambridge.

Short, K. C., and Stäublee, A.J. (1965). Outline of geology of Niger Delta:AmericanAssociation of Petroleum Geologists Bulletin, v. 51, p. 761-779.

Stacher, P. (1995). Present understanding of the Niger Delta hydrocarbon habitat, in, Oti, M.N., and Postma, G.,eds., Geology of Deltas: Rotterdam, A.A. Balkema, p. 257-267.

Todd, D.K. (1980). Groundwater Hydrology. 2nd edition, John Wiley, New York, 535 pp.

Ward, S. H. (1990a). Geotechnical and Environmental Geophysics, chapter Resistivity and Induced Polarization Methods, pages 147–189. Investigations in Geophysics No. 5. Soc.Expl. Geophys.

Whiteman, A. (1982).Nigeria: Its Petroleum Geology, Resources and Potential: London, Graham and Trotman, 394 p